

# Fracture Behavior of Rubber-Modified Injection Molded Poly(Butylene Terephthalate) with and without Short Glass Fiber Reinforcement

B. N. YOW,<sup>1</sup> U. S. ISHIAKU,<sup>1</sup> Z. A. MOHD ISHAK,<sup>1</sup> J. KARGER-KOCSIS<sup>2</sup>

<sup>1</sup> School of Industrial Technology, Universiti Sains Malaysia, 11800 Penang, Malaysia

<sup>2</sup> Institute for Composite Materials, University of Kaiserslautern, P.O. Box 3049, D-67663 Kaiserslautern, Germany

Received 27 February 2001; accepted 15 September 2001

**ABSTRACT:** Fracture behavior of poly(butylene terephthalate) (PBT) and its rubber-toughened (RT) 10 wt % grades; ethylene-co-glycidyl methacrylate-co-methacrylate terpolymer-toughened poly(butylene terephthalate) PBT/AX8900 (90/10), and Paraloid acrylic-based rubber-toughened poly(butylene terephthalate) PBT/EX2314 (90/10) was investigated using the fracture mechanics approach. The effects of controlling parameters such as type of impact modifier and deformation rate on fracture behavior of PBT and RT-PBT were investigated. Fracture tests were carried out on notched compact tension (CT) specimens. Fracture toughness,  $K_{Ic}$ , and fracture energy,  $G_c$ , of PBT decreased as the test speed increased from 1 to 500 mm/min. An opposite trend was observed in PBT/AX8900 and PBT/EXL2314. The fracture properties of 30 wt % short glass fiber-reinforced PBT (SGF-PBT) and 10 wt % impact-modified PBT composite (SGF-RT-PBT) were also studied. Incorporation of SGF into PBT has profoundly increased the fracture properties both at high and low speed. However, inclusion of 10 wt % of AX8900 into the reinforced PBT (PBT/AX8900/SGF) (60/10/30) adversely affected the fracture properties. EXL2314, on the other hand, showed a different effect, especially at high testing speed. Both types of impact modifiers were able to retain the flexural strength and flexural modulus of PBT. However, PBT/EXL2314 showed a better retention of flexural properties than PBT/AX8900. Incorporation of SGF in the EXL2314-toughened PBT, i.e., PBT/EXL2314/SGF (60/10/30) also gave a better balance of flexural properties compared to PBT/AX8900/SGF (60/10/30). Both PBT/AX8900 and PBT/EXL2314 showed enhancement of impact strength on the unnotched specimens. The failure modes of CT and impact specimens of PBT, RT-PBTs, and SGF-RT-PBTs were assessed using a scanning electron microscope (SEM). Brittle failure was observed for CT specimens of PBT at high testing speed, while incorporation of the impact modifier AX8900 and EXL2314 resulted in a shift of failure mode from brittle to ductile. SEM micrographs also revealed extensive fiber pull out in SGF-PBT and SGF-RT-PBT. © 2002 Wiley Periodicals, Inc. *J Appl Polym Sci* 84: 1233–1244, 2002; DOI 10.1002/app.10446

**Key words:** rubber-toughened; poly(butylene terephthalate); fracture; fiber-reinforced thermoplastics

## INTRODUCTION

The needs of plastics for engineering and other applications have been increasing for the past 3

decades. For some applications, improvement of the materials' fracture toughness must be met. This, at the same time, must be achieved without sacrificing the processibility and mechanical performance over a wide range of service temperature. Finally, the cost must be optimized. Basically, there are two approaches that have been recognized as routes to achieve these objectives. One is to produce a completely new polymer based

Correspondence to: Z. A. Mohd. Ishak (zarifin@usm.my).  
Contract grant sponsor: Universiti Sains Malaysia.

*Journal of Applied Polymer Science*, Vol. 84, 1233–1244 (2002)  
© 2002 Wiley Periodicals, Inc.

on a novel monomer, as in the case of polycarbonates (PC) and polysulphones.<sup>1</sup> The other route is by modification of the existing polymers such as incorporation of short glass fiber, block copolymer, structural foams, and rubbers.<sup>1</sup> Currently, there is growing interest in studies involving toughening of plastics by including rubber particles into the rigid matrix. The driving force behind this trend is the significant improvement in fracture resistance and better balance of properties than the parent polymer matrix. The studies of rubber-toughened plastics are vigorously carried out on commodity plastics; i.e., polystyrene (PS), acrylonitrile-butadiene-styrene (ABS), polymethylmethacrylate (PMMA), and polyvinylchloride (PVC) as well as engineering plastics; i.e., poly(ethylene terephthalate) (PET), polyamides (PA), and poly(butylene terephthalate) (PBT).<sup>2</sup> PBT is known for its good thermal, chemical, physical, electrical, and mechanical properties combined with satisfactory processing characteristics via short extrusion and injection molding cycles and excellent mold flow. However, it suffers one major drawback, i.e., it shows a strong tendency for brittle fracture when subjected to high-speed testing.

PBT shows relatively high unnotched impact strength in Izod test. However, the impact strength for notched Izod specimen is significantly low (2.5–3.0 kJ m<sup>-2</sup>).<sup>1</sup> Therefore, attempts are being made to enhance the fracture resistance of PBT by the including elastomeric impact modifiers so that the toughened PBT (RT-PBT) can meet the high impact performance requirement during service. Papers on rubber-toughened PBT are rather limited. Impact modifiers that are generally used for the studies can be grouped into two categories: one is core-shell type of impact modifier such as poly(methyl methacrylate)-grafted acrylate or butadiene rubber core,<sup>3</sup> and acrylate based core-shell type modified dispersed in a styrene/acrylonitrile (SAN) matrix.<sup>4–6</sup> These types of impact modifiers typically have a core of crosslinked butadiene or acrylic rubber and a shell of grafted chains that may physically interact with the ways that ensure good dispersion and coupling. The second category is blends with elastomeric materials, for example, acrylonitrile-butadiene-styrene (ABS),<sup>7–10</sup> butadiene-coacrylonitrile rubbers,<sup>11</sup> epoxidized ethylene propylene diene rubber (eEPDM),<sup>12</sup> and poly(ethylene-co-vinylacetate) (EVA).<sup>13</sup> Inclusion of rubber into the rigid thermoplastics to enhance the toughness of the subsequent system is, however, attained at

the expense of strength and stiffness. It is commonly known that the short glass fibers (SGF) with high aspect ratios are incorporated to improve the strength and stiffness of the polymer matrix. Therefore, SGF is incorporated into the rubber-toughened PBT in an attempt to achieve a material that has high stiffness, strength, and toughness to fulfill many high-performance applications' requirements. Literature publications in reinforced rubber-toughened composites are rather limited.<sup>2–12</sup>

## EXPERIMENTAL

### Material

The PBT used was a flame-retardant injection molding grade (Valox 310 SEO, GE Plastics, USA). The specific gravity is 1.39 g/cm<sup>3</sup>, and melt flow index ~7.02 g/10 min (load = 2.16 kg, 250°C). Two types of acrylate-based rubber as the impact modifiers viz. AX8900 was supplied by Atofina, Germany, while EXL2314 was supplied by Kureha Chemical Pte. Ltd, Singapore. AX8900 is ethylene-co-glycidyl methacrylate-co-methacrylate terpolymer (E/GMA/MA) that is comprised of 21–26 wt % acrylate and 6.5–8 wt % GMA. The melting point of AX8900 is 65°C, and the glass transition temperature is -40°C. Its melt flow index is 6 g/10 min. EXL2314 is comprised of alkyl acrylate, alkyl methacrylate, glycidyl methacrylate copolymer, which is an all-acrylic product. The melting point and glass transition temperature are 120 and -15°C, respectively. The bulk density is 0.43 ± 0.08 g/mL; 10 wt % of both acrylate rubbers was incorporated into the PBT matrix and considered as the RT-PBT material in this study, while RT-PBT containing 30 wt % SGF is designated as SGF-RT-PBT. The glass fiber with the trade name MaxiChop 3790 was supplied by PPG, Japan. The diameter and cut length of the glass fiber were 13 μm and 4 mm, respectively. It has a density of 2.65 g/cm<sup>3</sup>, and it was treated with silane.

### Processing

RT-PBT and SGF-RT-PBT were compounded using a HAAKE model counterrotating twin-screw extruder Rheomex CTW 100 using a speed of 22 rpm and temperature profile of 150–240°C from feeding zone to the die zone. The extrudate was pelletized with a HAAKE pelletizer. Film-gated

rectangular plaques of dimension  $149 \times 149 \times 3 \text{ mm}^3$  were injection molded from the pellets on a Battenflod Unilog 350CD injection molding machine. Melt and mold temperatures of 265 and 60°C, respectively, were used.

### Sample Characterization

The volume fraction of the fibers,  $V_f$  was determined by resin burnoff. The reinforced samples were pyrolyzed in a muffle furnace at 650°C, and this temperature was maintained until a constant weight was obtained. The fiber volume fraction was calculated from the following equation:

$$V_f = \frac{W_f/\rho_f}{W_f/\rho_f + W_m/\rho_m} \quad (1)$$

where  $V$  is the volume fraction,  $\rho$  is the density, and  $W$  is the weight: subscripts  $f$  and  $m$  refer to fiber and matrix, respectively. In the case of SGF-RT-PBT materials, the matrix refers to the toughened matrix.

A small portion of the fibers left behind after pyrolysis was dispersed in glycerol. A few drops of the dispersion were placed on a microscope slide. The slide was viewed under an optical microscope with a camera attachment. Photographs of various sections of the slide were taken to obtain a fair distribution of fibers. At least 500 fibers were measured from each batch. The number average fiber length,  $l_n$  and critical fiber length,  $l_c$  were calculated using eqs. (2) and (3) as follows:

$$l_n = \frac{\sum N_i l_i}{\sum N_i} \quad (2)$$

where  $N_i$  is the number of fibers of length  $l_i$ .

$$\left(\frac{l}{d}\right)_c = \frac{\sigma_{uf}}{2\tau_u} \quad (3)$$

where  $\sigma_{uf}$  is the ultimate fiber strength, which is 1500 MPa.  $\tau_u$  is the fiber–matrix interfacial shear strength. Assuming that the fibers are perfectly bonded, the interfacial shear strength becomes the shear strength of the polymer matrix, which is 53 MPa for PBT.<sup>14</sup> The diameter of the glass fiber,  $d$  is 13  $\mu\text{m}$ .

### Testing

Compact tension (CT) specimen with a notch length,  $a = 20 \text{ mm}$  and free ligament width,  $W$

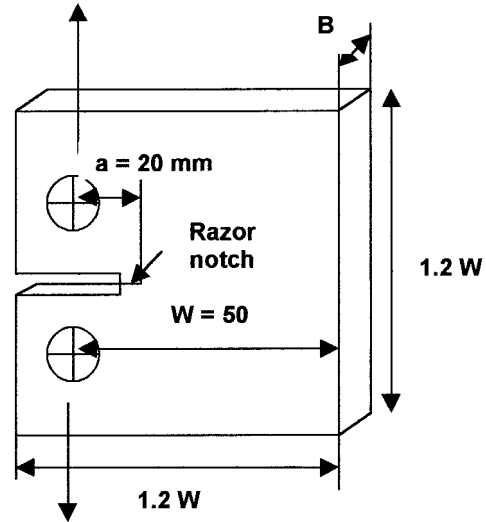


**Figure 1** Dimension of the compact tension specimen.

= 50 mm were machined from the injection molded plaques. Specimens with an initial notch cut transverse to the melt flow direction (MFD) were designated as  $L-T$  according to the ASTM E606-81 standard as shown in Figure 1. Prior to the tests the notches of the CT specimens were sharpened with a fresh razor blade. Fracture toughness determinations were performed on a Testometric testing machine. A crosshead speed of 1 and 500 mm/min were employed to investigate the effect of testing speed on the RT-PBTs and SGF-RT-PBTs. The fracture toughness ( $K_{Ic}$ ) and fracture energy ( $G_c$ ) were calculated in accordance with the recommendation of the Linear Elastic Fracture Mechanics (LEFM) standard.<sup>15</sup> In all cases, three CT specimens of each material were tested. Flexural test was also performed on a Testometric Testing machine in accordance to ASTM D790. Crosshead speeds of 1 and 500 mm/min with a span of 50 mm were employed. Five test specimens with  $12.70 \times 3.00 \text{ mm}$  (width  $\times$  thickness) were tested. Izod impact test was carried out according to ASTM D256 on a Zwick Pendulum machine on unnotched specimens with 63 mm in length, 3.00 mm in width, and 12.0 mm in thickness. A pendulum load of 7.5 J with a velocity of  $9.17 \text{ ms}^{-1}$  was employed.

### Conditioning of Specimens

Due to the hygroscopic nature of PBT, all test specimens were placed in a vacuum oven at 80°C for 24 h prior to testing. Upon removal from the

**Table I** The  $V_f$  and  $l_n$  of SGF-PBT and SGF-RT-PBT

	$V_f$	$l_n$ ( $\mu\text{m}$ )
PBT/SGF (70/30)	0.207	71.52
PBT/AX8900/SGF (60/10/30)	0.190	76.82
PBT/EXL2314/SGF (60/10/30)	0.196	78.83

oven, the specimens were allowed to cool to room temperature inside a desiccator.

### Fractography

The failure mode of the fractured CT and impact specimens was examined using a Leica Cambridge scanning electron microscope. SEM micrographs were taken at 10 kV acceleration voltage at various magnifications. Prior to the SEM observations the fractured parts were mounted on aluminum stub and sputter coated with a thin layer of gold to avoid electrical charging during examination.

## RESULTS AND DISCUSSION

### Volume Fraction of Fiber and Fiber Length Distribution

Table I shows the values of  $V_f$  and the number average fiber length,  $l_n$ , for the various PBT composites. It can be seen that the fiber lengths were degraded from their initial length of 4 mm. This can be attributed to attrition, which occurred dur-

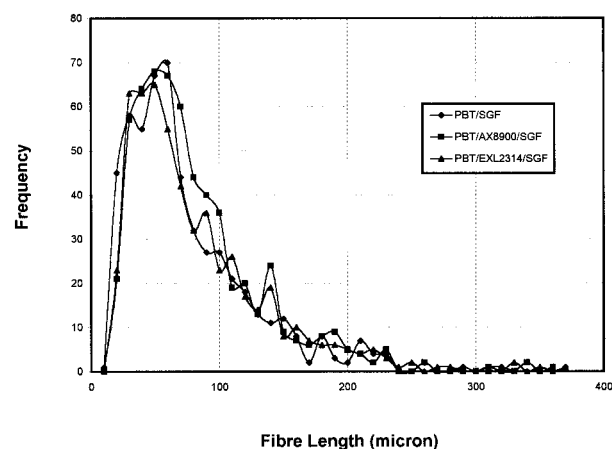


**Figure 2** Fiber length distribution of PBT/SGF (70/30), PBT/AX8900/SGF (60/10/30), and PBT/EXL2314/SGF (60/10/30).

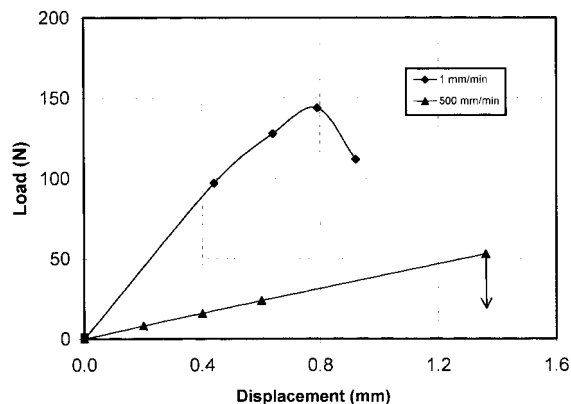


**Figure 3** Effect of test speed on the load-displacement curve for PBT/AX8900 (90/10).

ing processing via twin-screw extruder and injection molding. The possible attrition that contributed to the breakage of the fibers<sup>16</sup> includes fiber-fiber interaction, fiber-polymer melt interaction, and also the fiber-processing cylinder contact. Lunt and Shortall<sup>17</sup> observed that most of the fiber breakage occurred at the solid melt interfaces, where high shear stresses were encountered as a result of both the temperature and velocity gradients in their study on the extrusion compounding of short glass fiber reinforced nylon 6.6.

The critical fiber length,  $l_c$ , calculated using eq. (3) is 188.63  $\mu\text{m}$ . The energy required for the fiber to debond and pull out completely from the matrix, is maximum when the fiber length equals to  $l_c$ .<sup>18</sup> The fiber length distribution (FLD) for PBT/SGF, PBT/AX8900/SGF, and PBT/EXL2314/SGF is shown in Figure 2. It is indicated that most of the fibers are distributed below the  $l_c$ .

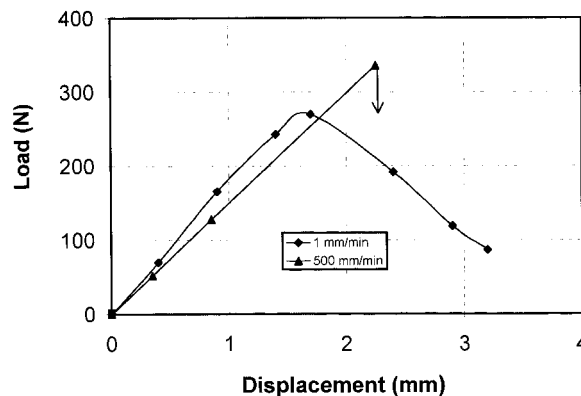


**Figure 4** Effect of test speed on the load-displacement curve for PBT/AX8900 (90/10).



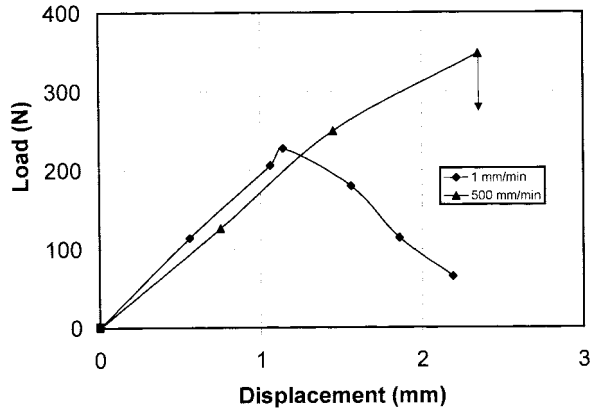


**Figure 5** Effect of test speed on the load–displacement curve for PBT/EXL2314 (90/10).

### Fracture Test

Figures 3–4 show the effect of test speed on the load vs. deflection curve for PBT, PBT/AX8900, and PBT/EXL2314, respectively. It can be seen in Figure 3 that PBT broke at rather low deflection when the test speed increased. Lower load was also detected when PBT was subjected to high testing speed. The catastrophic breakage of test specimen was also observed in PBT/AX8900 and PBT/EXL2314 when it was subjected to high testing speed. However, the load–deflection curves (Figs. 4 and 5) of RT-PBT tested at high speeds showed similarity at the initial curve but indicated rather higher load at peak. This was not obtained in the case of PBT tested at high speed, i.e., 500 mm/min. Furthermore, the difference of load at peak between specimens tested at low and high speed was more apparent in PBT/EXL2314. This explained the results obtained for  $K_c$  and  $G_c$  values of PBT/EXL2314 tested at 1 and 500 mm/min (Table II).

Table II shows the effect of test speed on fracture toughness,  $K_c$  of PBT and its RT-PBT counterpart. PBT is a semicrystalline thermoplastic which is the mechanical response and, thus failure is frequency dependent, due to the segmental mobility of the macromolecules.<sup>19</sup> From Figure 8,  $K_c$  values of PBT decreased as the test speed increased from 1 to 500 mm/min. The embrittlement is attributed to the inability of PBT to undergo plastic deformation in the form of crazing and shear yielding when subjected to high-speed deformation. Both fracture parameters,  $K_c$  and  $G_c$  are strongly affected by the deformation rate. Similar observations were reported for other engineering thermoplastics.<sup>1,19</sup> From Table II, it can be seen that a similar trend is also observed in the case of fracture energy,  $G_c$ , of PBT. However, an opposite trend is observed for both RT-PBTs, i.e., PBT/AX8900 and PBT/EXL2314 where both  $K_c$  and  $G_c$  values did not decrease as the deformation rate increased. At a low deformation rate, both AX8900 and EXL2314 enhanced both fracture parameters,  $K_c$  and  $G_c$  of the parent matrix, PBT. However, the toughness enhancement is more conspicuous when the materials were subjected to high-speed deformation. At a test speed of 500 mm/min, both PBT/AX8900 and PBT/EXL2314 showed excellent improvement in the fracture toughness,  $K_c$ , i.e., 420 and 480%, respectively. This indicates that the inclusion of AX8900 and EXL2314 has effectively toughened the PBT matrix. Due to the shear yielding behavior of the PBT matrix, it is suggested that the modifiers have toughened the PBT by inducing energy dissipation mechanisms in the form of crazing and shear yielding processes in the matrix.<sup>1</sup> Cecero et al.<sup>20</sup> also suggested that the rubber particle acts as a stress concentrator that favors the dissipa-

**Table II**  $K_c$  and  $G_c$  Values for RT-PBT and SGF-RT-PBT Tested at 1 and 500 mm/min

Test Speed (mm/min)	$K_c$ (MPam <sup>1/2</sup> )		$G_c$ (kJ/m <sup>2</sup> )	
	1	500	1	500
RT-PBT				
PBT (100/0)	1.72	0.66	2.47	1.00
PBT/AX8900 (90/10)	3.00	3.43	9.02	11.43
PBT/EXL2314 (90/10)	2.55	3.84	6.23	16.26
SGF-RT-PBT				
PBT/SGF (70/30)	3.35	1.81	4.82	4.21
PBT/AX8900/SGF (60/10/30)	3.40	1.89	6.53	3.63
PBT/EXL2314/SGF (60/10/30)	3.06	2.82	3.84	5.01

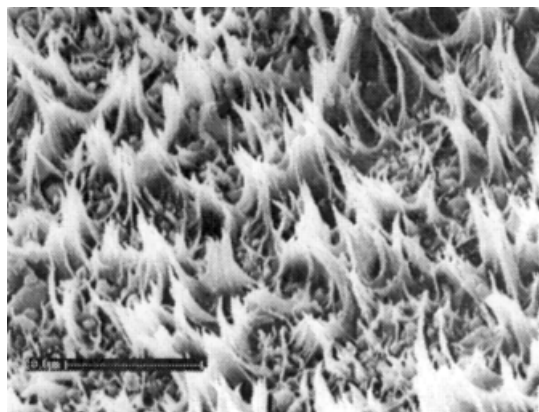


**Figure 6** SEM micrograph of PBT (100/0) compact tension specimen tested at 1 mm/min (3K x).

tion of impact energy. Shear yielding in PBT matrix is evident from the polymer fibril formed as a result of the drawing of the matrix (Fig. 6). The rubber particles are believed to be responsible for initiating the shear yielding.<sup>21</sup> Apart from this, the shear bands also present a barrier to the propagation of crazes, and hence, crack growth,<sup>1</sup> subsequently, delaying the failure of the material. Similar observations were also reported by Cruz et al.<sup>22</sup> on methacrylate–butadiene–styrene (MBS) core shell-modified PBT, Hourston et al.<sup>23</sup> on PBT-(butadiene-*co*-acrylonitrile) blends, and also Wang et al.<sup>12</sup> on epoxidized ethylene propylene diene toughened PBT.

It is also noted from Table II that the incorporation of SGF into PBT matrix enhanced the fracture parameters  $K_c$  and  $G_c$  of the system tested

under both speeds, i.e., 1 and 500 mm/min. This is because most of the fibers in the system are shorter than the critical length,  $l_c$ . Therefore, the improvement in fracture toughness can be attributed to the better energy dissipation ability of the system through combination of fiber related micromechanisms such as fiber bridging, pull out, and work done against friction in pulling the fibers out of the matrix.<sup>18</sup> Similar results were reported by Mohd Ishak et al. on fiber-reinforced core-shell rubber-modified PBT (CSR-PBT)<sup>4</sup> and short fiber-reinforced polyarylamide (PAR).<sup>24</sup> However, fracture analysis on the SGF-RT-PBTs, which employed AX8900 as the impact modifier in the PBT composite, i.e., PBT/AX8900/SGF (60/10/30), showed a insufficient improvement in  $K_c$  (3.40 MPam<sup>1/2</sup>) and  $G_c$  (6.53 kJ/m<sup>2</sup>) values at the test speed of 1 mm/min. The percentage increase of  $G_c$  value (35.5%) is rather higher than that of  $K_c$  value (1.5%). However, at high deformation rate, i.e., 500 mm/min, both  $K_c$  and  $G_c$  values of PBT/AX8900/SGF decreased, and are lower compared to the untoughened PBT composite. This indicates that the inclusion of impact modifier, AX8900 into the SGF-reinforced PBT matrix failed to present a synergistic effect on the toughness of the system under high-speed testing. This is in contrast to PBT composite toughened with EXL2314 where a synergistic effect is exhibited. It can be seen in Table II that the values of  $K_c$  and  $G_c$  are higher than those of PBT/SGF tested at 500 mm/min, although a slight decrease of the values are observed at low testing speed, i.e., 1 mm/min.

**Table III** Flexural Properties of RT-PBT and SGF-RT-PBT Tested at 1 and 500 mm/min

Test Speed (mm/min)	Flexural Strength (MPa)		Flexural Modulus (GPa)	
	1	500	1	500
<b>RT-PBT</b>				
PBT (100/0)	83.8	79.6 (−5.0)	2.7	2.8 (+1.1)
PBT/AX8900 (90/10)	66.3	71.5 (+1.6)	2.0	2.1 (+9.0)
PBT/EXL2314 (90/10)	79.9	91.1 (+14.0)	2.3	2.1 (−7.5)
<b>SGF-RT-PBT</b>				
PBT/SGF (70/30)	113.5	131.2 (+16.2)	6.1	7.7 (+26.9)
PBT/AX8900/SGF (60/10/30)	63.4	79.8 (+36.4)	3.2	4.2 (+29.8)
PBT/EXL2314/SGF (60/10/30)	84.9	94.9 (+11.8)	4.7	5.8 (+22.9)

( ) % changes as compared to that of 1 mm/min.

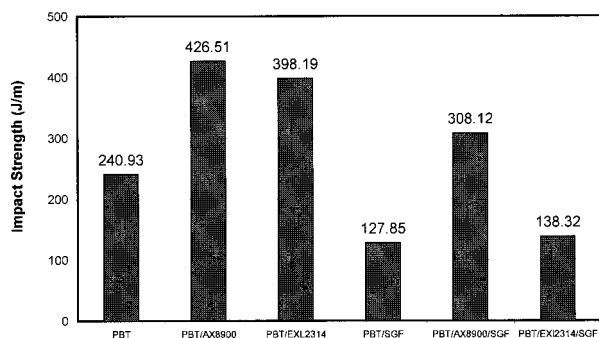
+ Increase.

− Decrease.

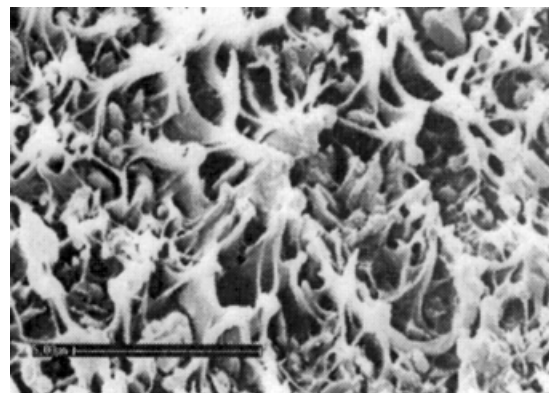
## Flexural Test

Table III shows the flexural strength and flexural modulus of PBT, RT-PBT, and SGF-RT-PBT tested at 1 and 500 mm/min. It can be seen that irrespective of test speed, the incorporation of either AX8900 or EXL2314 deteriorated the flexural properties. However, better retention in flexural properties is displayed by PBT/EXL2314. A higher retention of 95 and 85% of the flexural strength and flexural modulus, respectively, were recorded of the neat PBT in the presence of EXL2314. In the case of PBT/AX8900, percentage retention of 79 and 72% was recorded for flexural strength and flexural modulus, respectively. The drop of the flexural properties can be attributed to the lower modulus and strength of the acrylic based modifiers. A similar result was reported for SAN acrylate based core-shell rubber (CSR)-toughened PBT.<sup>4,5</sup>

As expected, incorporation of 30 wt % SGF into the PBT matrix increased both the flexural strength and flexural modulus. It is definite that the enhancement in the flexural strength is attributed to the reinforcement of glass fiber with a high aspect ratio. Percorini and Herzberg<sup>25</sup> and Mohd Ishak et al.<sup>4</sup> reported similar results on rubber-toughened short glass fiber nylon 6.6 composites and short glass fiber-reinforced CSR-PBT, respectively. The inclusion of 10 wt % of either AX8900 or EXL2314 into the SGF-reinforced PBT adversely affected the flexural properties. Even then, the flexural strength is comparable to the corresponding toughened grades (RT-PBTs). However, the flexural strength of the SGF-RT-PBTs increased when it was subjected to high testing speed. As for the flexural modulus, incorporation of SGF yielded 122 and 178% enhance-



**Figure 7** Unnotched Izod impact strength of PBT, PBT/AX8900, PBT/EXL2314, PBT/SFG, PBT/AX8900/SFG, and PBT/EXL2314.



**Figure 8** SEM micrograph of PBT (100/0) compact tension specimen tested at 500 mm/min (8K x).

ment when test specimen subjected to 1 and 500 mm/min testing speed, respectively. With the incorporation of 10 wt % of AX8900 and EXL2314 was incorporated into the PBT composite, the flexural modulus dropped similarly as in flexural strength. The retentionability of flexural properties is, however, better in the EXL2314-toughened PBT composites compared to AX8900-toughened PBT composites. This is in agreement with the trend observed earlier in the case of RT-PBTs. It is also found that unlike fracture properties (Table II), the flexural properties of both the RT-PBT and SGF-RT-PBT are not significantly affected by the test speed. The variation in flexural strength ranged from a maximum increase 36.4% and a decrease of 5.0% compared to flexural modulus, which showed 29.8 and 7.5%, respectively.

## Izod Impact Test

In Figure 7, the impact strength of unnotched PBT, SGF-PBT, RT-PBT, and SGF-RT-PBT specimens are compared. It shows that incorporation of 10 wt % of impact modifiers AX8900 and EXL2314 enhanced the impact strength of the unnotched samples. This can be attributed to the contribution of the impact modifier in energy absorption during the impact.

PBT/SGF somehow shows a very much lower unnotched impact strength, i.e., about 50% lower than that of neat PBT. This indicates that the incorporation of SGF has restricted the plastics deformation of the matrix. As the result of the micromechanical constraint imposed by the fibers, energy absorbed during impact is readily reduced. It is also noted that the inclusion of 10 wt % of AX8900 into the reinforced PBT matrix



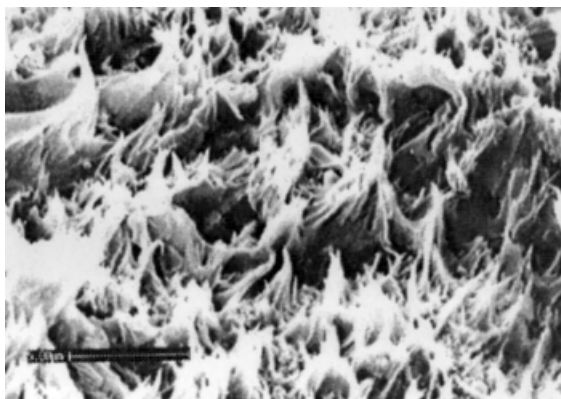


**Figure 9** SEM micrograph of PBT/AX8900 (90/10) compact tension specimen tested at 1 mm/min (5K x).

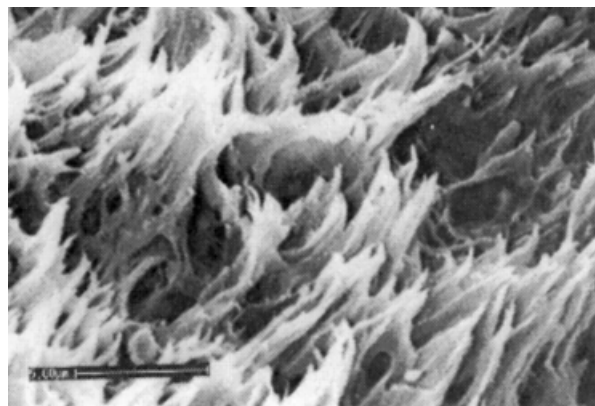


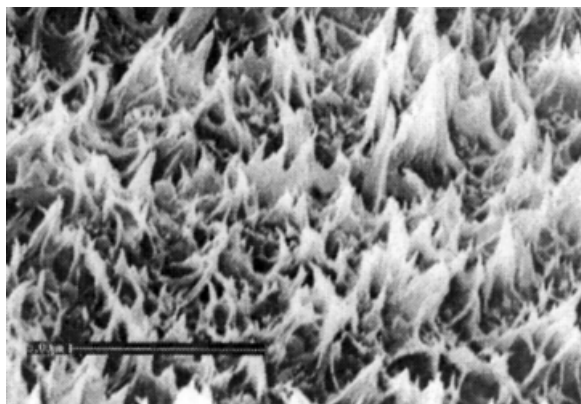
**Figure 11** SEM micrograph of PBT/EXL2314 (90/10) compact tension specimen tested at 500 mm/min (5K x).

improved the impact strength significantly, and it is higher than that of neat PBT, although it is lower than the corresponding rubber-toughened system, i.e., PBT/AX8900. EXL2314-modified PBT composite, on the other hand, showed only a slight improvement in the unnotched impact strength compared to the toughened system, i.e., PBT/EXL2314. However, the impact strength is still inferior to that of the neat PBT matrix (Fig. 7). Inclusion of 10 wt % AX8900 seemed to be able to restore some form of rubber debonding from the matrix. It is evident from the rather rough fracture surface as shown in SEM micrographs, which will be revealed in the next section. Sheathed debonded fibers are also observed on the fracture surface.

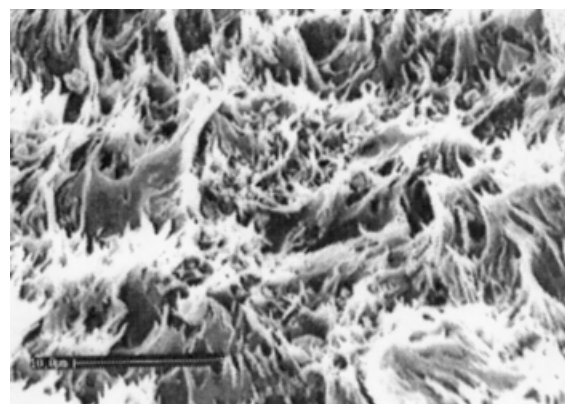
#### Fractography Study

Figure 6 shows the SEM micrograph of the CT specimen of PBT tested at 1 mm/min. The draw-

ing of matrix or so-called shear yielding, which is believed to be responsible for the ductility of PBT, is manifested by the fibrils formed. However, the segmental mobility that induces shear yielding is rather limited at high-speed deformation. It is evident from Figure 8 where the fibrils caused by drawing of matrix became less prominent. Figures 9 and 10 show the effect of modifier inclusion, i.e., AX8900 and EXL2314, respectively, on the fracture surface of PBT that were tested at 1 mm/min. It can be seen that there is extensive plastic deformation on the fracture surface. Rubber cavitation is believed to be the inducer to the multiple crazing and shear yielding, hence, enhanced the toughness of the modified PBT. This consequently leads to higher  $K_c$  and  $G_c$  values (Table II). The toughening effect of the modifier EXL2314 is still prominent at high test speed, i.e., 500 mm/min as indicated in Figure 11. The extensive fibrillation implies that the energy absorbing



**Figure 10** SEM micrograph of PBT/EXL2314 (90/10) compact tension specimen tested at 1 mm/min (8K x).



**Figure 12** SEM micrograph of PBT/AX8900 (90/10) compact tension specimen tested at 500 mm/min (3K x).



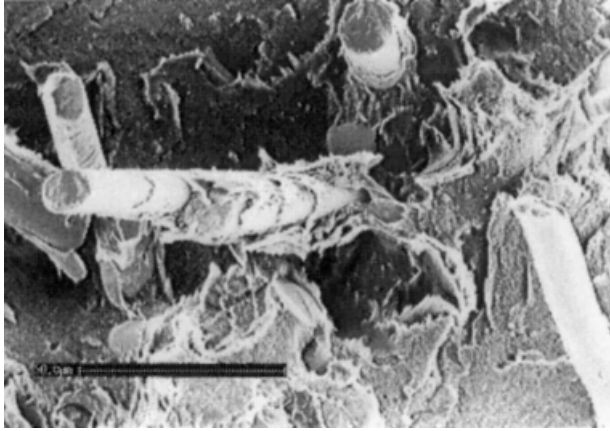


**Figure 13** SEM micrograph of PBT/SGF (70/30) compact tension specimen tested at 1 mm/min (800 x).

mechanism in the presence of modifier EXL2314 is more favorable at high-speed deformation. Modifier AX8900 also exhibited a similar effect at high test speed. However, it can be noted from Figure 12, that fibrillation of the matrix seemed to be less prevalent than that of PBT/EXL2314. This explains the lower percentage of increase in  $K_c$  and  $G_c$  values of PBT/AX8900 tested at 500 mm/min.

Figures 13 and 14 show the fracture surface of PBT/SGF (70/30) tested at 1 and 500 mm/min, respectively. Extensive fiber pull out is manifested on the fracture plane. Fiber pullout has been observed in various short fiber-reinforced thermoplastics<sup>17,26,28</sup> as the dominant failure mechanism. A comparison of the fracture surface of PBT/SGF (Fig. 13) and PBT (Fig. 6) reveals that the incorporation of SGF has reduced the

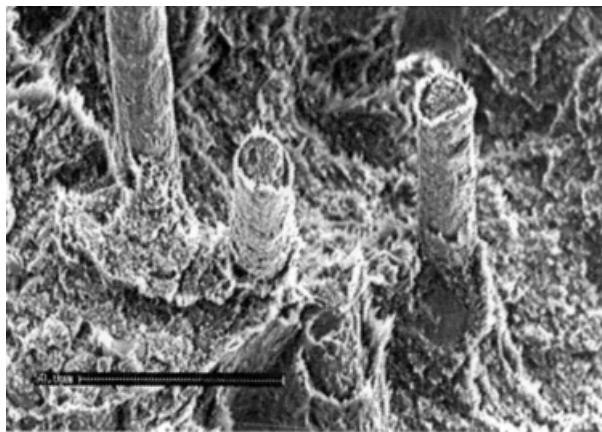


**Figure 14** SEM micrograph of PBT/SGF (70/30) compact tension specimen tested at 500 mm/min (800 x).



**Figure 15** SEM micrograph of PBT/AX8900/SGF (60/10/30) compact tension specimen tested at 1 mm/min (700 x).

deformation of the PBT matrix. This can be attributed to the micromechanical constraint imposed by the fibers. The fibers pulled out are bare on the surface. Mohd Ishak et al.<sup>4</sup> also reported a similar observation on PBT composites. A different observation was obtained with PBT composite tested at 500 mm/min. The fibers pulled out are sheathed with deformed PBT matrix (Fig. 14). This indicates that the fiber–matrix adhesion is better at a lower test speed. Karger-Kocsis<sup>29</sup> explained that the formation of sheathed pullout can be attributed to the smaller shear strength of the matrix due to the rubber modification. Gaymans<sup>30</sup> also attributed this sheathed pullout to the onset of cavitation. This also suggests that the interfacial debonding occurred but the lower  $K_c$

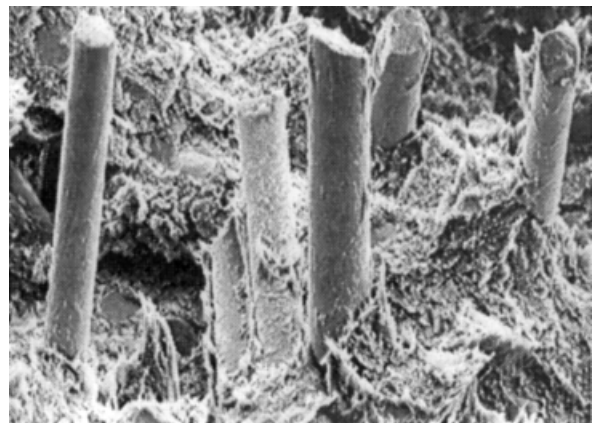


**Figure 16** SEM micrograph of PBT/AX8900/SGF (60/10/30) compact tension specimen tested at 500 mm/min (800 x).

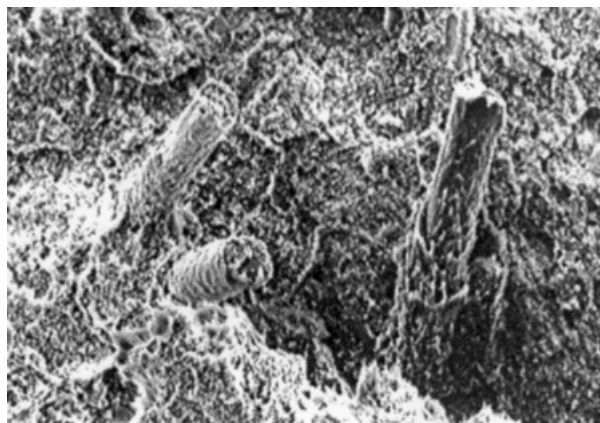


**Figure 17** SEM micrograph of PBT/EXL2314/SGF (60/10/30) compact tension specimen tested at 1 mm/min (800 x).

and  $G_c$  values reported indicate that the failure mechanism is not effective in enhancing the toughness of PBT at high deformation rate. The PBT sheath on the fiber surface is also displayed on the rubber modified PBT composites, i.e., PBT/AX8900/SGF (60/10/30) and PBT/EXL2314/SGF (60/10/30) tested at 1 and 500 mm/min (Figs. 15–18). However, the formation of sheathed layer on the fiber surface is more extensive in the case of PBT/EXL2314/SGF (Figs. 17 and 18) compared to that of PBT/AX8900/SGF (Figs. 15 and 16). Several studies<sup>28,30,31</sup> on rubber-toughened PA composites reported that the thickness of the sheathed layer increased with rubber concentration, temperature, and deformation rate. Extensive fiber pullout and matrix fibrillation are noticed on the fracture planes of SGF-RT-PBTs.

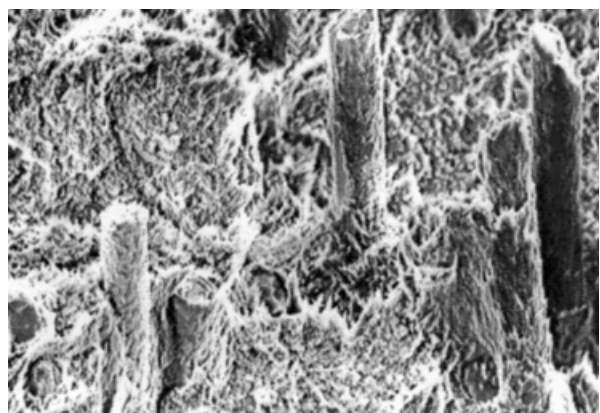


**Figure 18** SEM micrograph of PBT/EXL2314/SGF (60/10/30) compact tension specimen tested at 500 mm/min (700 x).

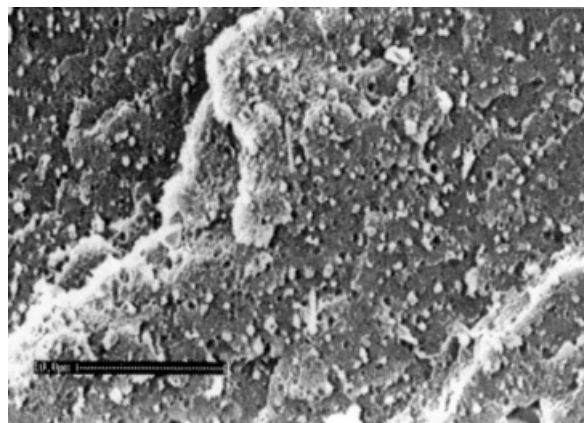


**Figure 19** SEM micrograph of PBT (100/0) unnotched Izod specimen (3K x).

This is an indication that the deformation of PBT matrix is still prevalent in the PBT composites. The effectiveness of the EXL2314 in inducing shear yielding of PBT matrix became more apparent under high testing speed (Fig. 18). This leads to the formation of a large damage zone, which subsequently enhanced  $K_c$  and  $G_c$  values. An extensive review by Walker and Collyer<sup>19</sup> suggests that the effectiveness of rubber particle in improving the toughness of thermoplastics matrices is strongly controlled by their ability to act as stress concentrating sites to induce multiple energy and shear yielding. Figure 15 evidence for the inferior ability of AX8900 to induce shear yielding ability compared to EXL2314 (Figs. 17 and 18). This perhaps explains the lower  $G_c$  and  $K_c$  values obtained for PBT/AX8900/SGF tested at high test speed, i.e. 500 mm/min (Table II).

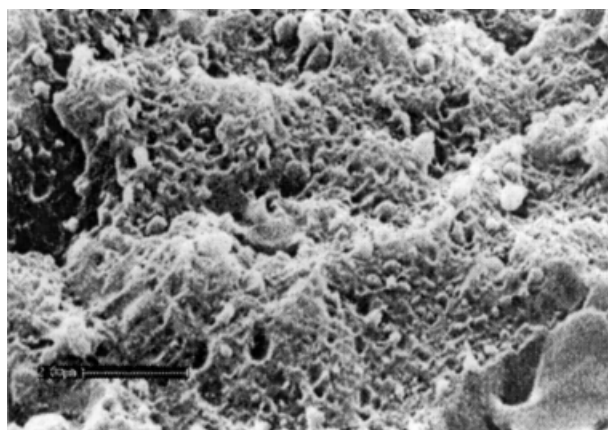


**Figure 20** SEM micrograph of PBT/AX8900 (90/10) unnotched Izod specimen (10K x).



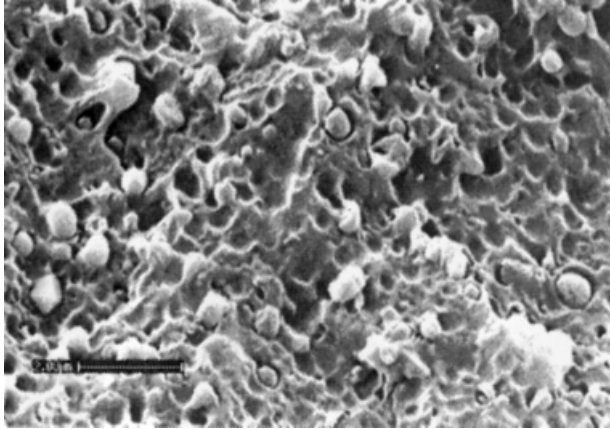


**Figure 21** SEM micrograph of PBT/EXL2314 (90/10) unnotched Izod specimen (10K x).

Figures 19–24 are SEM micrographs of impact test specimens. As can be seen in Figure 19, the fracture surface of the unnotched PBT specimen shows a brittle failure mode. Similar observations were obtained for PBT/AX8900 (Fig. 20) and PBT/EXL2314 (Fig. 21). The finer dispersion of the AX8900 compared to that of EXL2314 (Figs. 20 and 21) is believed to lead to higher impact strength of AX8900 modified PBT (Fig. 7). Extensive fiber pull out is observed in the fracture surfaces of the unnotched Izod impact specimens (Figs. 22–24). Sheathed fibers pulled out were only observed in SGF-RT-PBTs (Figs. 23 and 24). It can be noted that the SGF-RT-PBTs' fracture surfaces are rather rough compared to the un-toughened PBT composites.

## CONCLUSION

Fracture analysis results showed that the fracture toughness of PBT improved with the incor-

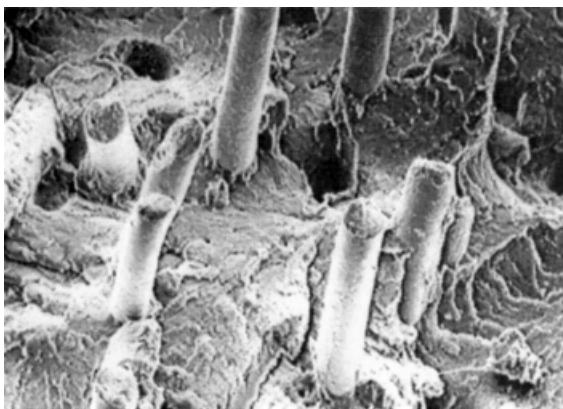


**Figure 22** SEM micrograph of PBT/SGF (70/30) unnotched Izod specimen (800 x).

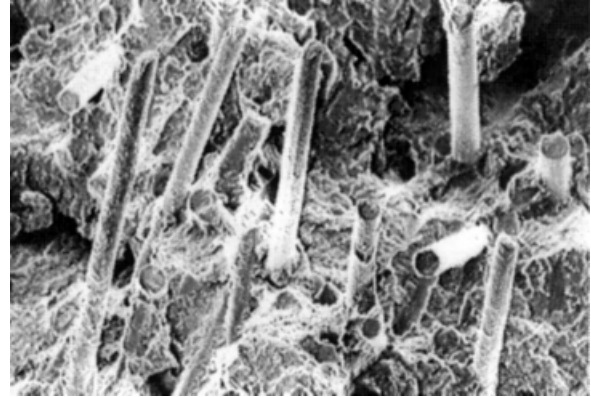


**Figure 23** SEM micrograph of PBT/AX8900/SGF (60/10/30) unnotched Izod specimen (400 x).

poration of 10 wt % of either AX8900 or EXL2314. PBT/EXL2314/SGF exhibited better fracture toughness at high test speed while PBT/AX8900/SGF showed higher toughness at low test speed. Flexural properties deteriorated with the incorporation of both AX8900 and EXL2314. The incorporation of either AX8900 or EXL2314, on the other hand, improved the unnotched Izod impact strength significantly. The flexural properties improved when SGF was introduced in the rubber-modified PBT matrix. However, the contrary was observed in the case of the impact strength. SEM micrographs revealed that a shift of failure mode from tough to a brittle one in PBT occurred when it was tested at 500 mm/min. Transition of failure mode was not apparent in PBT/AX8900 and PBT/EXL2314. The ternary system, i.e., PBT/AX8900/SGF and PBT/EXL2314/SGF showed a combination of both plastic deformation and fiber pullout

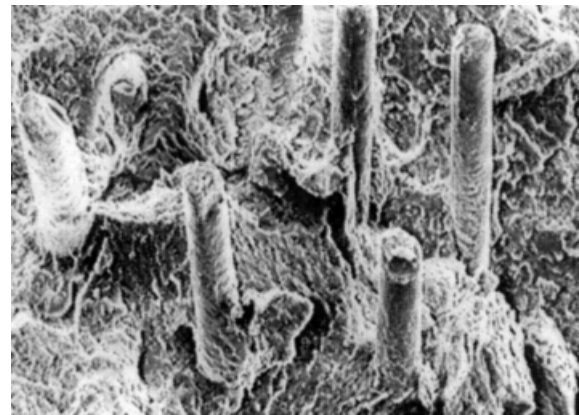


**Figure 24** SEM micrograph of PBT/EXL2314/SGF (60/10/30) unnotched Izod specimen (700 x).

as the dominant energy absorbing mechanism. Sheathed fiber pullout was also observed.

The authors would like to present their appreciation to Universiti Sains Malaysia for the financial support on this project. We are also thankful to Professor J. Karger-Kocsis, from IVW, Kaiserslautern, Germany, Dr. C. A. Cruz Jr., from Rohm & Haas Company, USA, and Mr. Ved Sahajpal from Kureha Chemical, Singapore, for supplying the impact modifiers used in this study. The assistance of Mr. Ryuji Kobayashi from PPG, Japan, by providing the short glass fiber for the study is well appreciated.

## REFERENCES

- Bucknall, C. B. *Toughened Plastics*; Applied Science: London, 1977.
- Savadori, A. In *Rubber Toughened Engineering Plastics*; Collyer, A. A., Ed.; Chapman & Hall: London, 1994.
- Brady, A. J.; Keskkula, H.; Paul, D. R. *Polymer*, 1994, 35, 3665.
- Mohd. Ishak, Z. A.; Ishiaku, U. S.; Karger-Kocsis, J. *Comp Sci Technol* 2000, 60, 803.
- Mohd. Ishak, Z. A.; Ishiaku, U. S.; Karger-Kocsis, J. *J Appl Polym Sci* 1999, 74, 2470.
- Czigany, T.; Mohd. Ishak, Z. A.; Heitz, T.; Karger-Kocsis, J. *Polym Comp* 1996, 17, 900.
- Hale, W.; Keskkula, H.; Paul, D. R. *Polymer*, 1999, 40, 3353.
- Hage, E.; Hale, W.; Keskkula, H.; Paul, D. R. *Polymer*, 1997, 38, 3237.
- Hale, W.; Keskkula, H.; Paul, D. R. *Polymer*, 1999, 40, 365.
- Hale, W.; Keskkula, H.; Paul, D. R. *Polymer*, 1999, 40, 3665.
- Hourston, D. J.; Lane, S.; Zhang, H. X. *Polymer*, 1995, 36, 3051.
- Wang, X. H.; Zhang, H. X.; Wang, Z. G.; Jiang, B. Z. *Polymer*, 1997, 38, 1569.
- Francesco, P.; Pezzin, G. *Polym Eng Sci* 1984, 24, 618.
- General Electric Company. *VALOX PBT Resin Product Guide*; 1997, p. 11.
- Williams, J. G. *A Linear Elastic Fracture Mechanics (LEFM) Standard for Determining  $K_{Ic}$  and  $G_c$  for Plastics*; Mech. Eng. Dept., Imperial College, London, UK, 1988.
- Turkovich, R. V.; Erwin, L. *Polym Eng Sci* 1986, 32, 2989.
- Lunt, J. M.; Shortall, J. B. *Plast Rubber Process Appl* 1979, 5, 37.
- Karger-Kocsis, J.; Friedrich, K. In *Solid State Behavior of Linear Polyesters and Polyamides*; Schultz, J. M.; Fakirov, S., Eds.; Prentice Hall Inc.: Englewood Cliffs, NJ, 1990, p. 249.
- Walker, I.; Collyer, A. A. In *Rubber Toughened Engineering Plastics*; Collyer, A. A., Ed.; Chapman & Hall: London, 1994.
- Cecero, A.; Greco, R.; Ragosta, G.; Scarinzi, G.; Tagliatela, A. *Polymer*, 1990, 31, 1239.
- Cruz, C. A., Jr.; Havrilik, S. J., Jr. *Impact Behavior and High Speed Tensile Testing in Toughened PBT*; *Plastics Additives Research Dept.*, Rohm & Haas Company, USA, 1997.
- Cruz, C. A., Jr.; Havrilik, S. J., Jr.; Slavin, S. *Fracture and Viscoelastic Aspect of PBT Toughening With A Core/Shell Modifier*; *Plastics Additives Research Dept.*, Rohm & Haas Company, USA, 1997.
- Hourston, D. J.; Lane, S.; Zhang, H. X. *Polymer*, 1991, 32, 2215.
- Mohd. Ishak, Z. A.; Ishiaku, U. S.; Karger Kocsis, J. *J Mater Sci* 1998, 33, 3377.
- Pecorini, T. J.; Hertzberg, R. W. *Polym Comp* 1994, 15, 174.
- Folkes, M. J. *Short Fiber Reinforced Thermoplastics*; *Research Studies Press*, John Wiley: Chichester, UK, 1982.
- Seiler, E.; Porst, H. G.; Theysohn, K. *5th Eur. Plast. Rubb. Conf.*, Paris, 1978.
- Mohd. Ishak, Z. A.; Lim, N. C. *Polym Eng Sci* 1994, 34, 1645.
- Karger-Kocsis, J. In *Polymer Blends: Formulations And Performance*; Paul, D. R.; Bucknall, C. B., Eds.; John Wiley & Sons Inc., New York, 1998.
- Gaymans, R. J. *Toughened Polyamides*. In *Rubber Toughened Engineering Plastics*; Collyer, A. A., Eds.; Chapman & Hall, London, 1994.
- Bailey, R. S.; Baden, M. G. In *Applied Fracture Mechanics to Composite Materials*; Friedrich, K., Ed.; Amsterdam: Elsevier, 1989.